Separation Science and Technology
Publication details, including instructions for authors and subscription information:
http://www.informaworld.com/smpp/title~content=t713708471

Theory of Isotope Separation by Electrochemical Parametric Pumping

Yoram Oren[a]; Abraham Soffer[a]
[a] NUCLEAR RESEARCH CENTRE-NEGEV, BEER-SHEVA, ISRAEL

To cite this Article Oren, Yoram and Soffer, Abraham(1984) 'Theory of Isotope Separation by Electrochemical Parametric Pumping', Separation Science and Technology, 19: 8, 575 — 602
To link to this Article: DOI: 10.1080/01496398408060336
URL: http://dx.doi.org/10.1080/01496398408060336

SEPARATION SCIENCE AND TECHNOLOGY, 19(8 & 9), pp. 575-602, 1984

Theory of Isotope Separation by Electrochemical Parametric Pumping

YORAM OREN and ABRAHAM SOFFER

NUCLEAR RESEARCH CENTRE—NEGEV
BEER-SHEVA 84190, ISRAEL

Abstract

Electrochemical parametric pumping is a novel separation process in which cycles of reversible electrochemical processes on high surface area electrodes are conducted in synchronization with cycles of solution flow through the separating column. In the present work, isotope separation by electrochemical parametric pumping is studied theoretically. The proposed model is based on the similarity between the parametric pumping and the countercurrent processes and on the division of the separating column to "cells" when dispersion processes are neglected. Steady-state isotopic concentration gradients are calculated and process optimization is performed with respect to system parameters such as the fraction of the isotopes bound to the electrode, the solution displacement volume, and the fraction of the isotopes withdrawn as product. The model may also be applicable to other types of parametric pumping.

1. INTRODUCTION

The concept of electrochemical parametric pumping (ECPP) was introduced by us previously (*1–3*). It was shown that a high degree of separation of salt from water (desalination) can be induced by cycles of electroadsorption and electrodesorption of the salt on and from the electrical double layer region of a couple of high surface area porous carbon electrodes. These processes, when properly synchronized with periodical changes of solution flow direction, result in a considerable salt concentration gradient along the desalination column.

The equilibrium and dynamic properties of the ECPP were treated theoretically and the model proposed for the two components ($NaCl–H_2O$)

 0149-6395/85/1908-0575$3.50/0

separation process was in a good agreement with the experimental results, particularly when interphase equilibrium was maintained (*3*).

The ECPP is attractive also for the separation of ions, isotopes, or minute quantities of uncharged species. The properties which may lead to separation in these systems are differences in redox potentials (*4, 5*), the existence of isotope effects in electroadsorption or electrodeposition (*6*), and differences in electroadsorption tendencies of neutral organic species due to dipole-charge interactions (*7*).

The importance of separation of multicomponent mixtures and isotopes is not controversial. However, the application of the parametric pumping concept to these systems has been considered in only a few publications. Butts, Gupta, and Sweed (*8*) extended the idea of equilibrium parametric pumping established by Pigford, Becker, and Blum (*9*) to multicomponent systems. Chen et al. (*10*) separated toluene–aniline and *n*-heptane by thermal parametric pumping on silica gel and also presented an equilibrium theory assuming that the multicomponent mixture contains a series of pseudobinary systems. Recently Wu and Wankat (*11*) studied the separation of pyrene from acenaphthylene by thermal parametric pumping.

The separation of isotopes by parametric pumping was considered only in two works: Weaver and Hamrin (*12*) separated hydrogen isotopes in the gas phase by using a process scheme similar to the parametric pumping; Schroeder and Hamrin (*13*) separated boron isotopes by direct mode thermal parametric pumping and obtained relatively small elementary separation factors (1.02 to 1.028).

In the present paper, isotope separation by the ECPP scheme is treated theoretically. The theory is based on the similarity between the parametric pumping and the countercurrent separation processes, an idea that was first presented by Grevillot and Tondeur (*14*) for thermal parametric pumping.

2. MODEL OUTLINE

2.1. Electrochemical Considerations

Isotope separation by ECPP is due to the existence of an isotope effect when an isotopic mixture of a dissolved electroactive element is bound to an electrode by an electrochemical process. For a mixture of two isotopes, a and b, the process is characterized by a separation factor defined as

$$\alpha = \frac{Z}{1-Z} \Big/ \frac{Zs}{1-Zs} \tag{1}$$

where Z and Zs are the mole fractions of Isotope a in the solution and on the electrode, respectively. In the following discussion we shall consider Isotope b to be preferentially bound to the electrode; thus, $\alpha > 1$.

As in the case of water desalination, the ECPP unit for isotope separation will contain a working (separating) electrode upon which the desired electrochemical separation process occurs and an auxiliary electrode which must be either separated (e.g., by an ion-exchange membrane) or involved in reactions which do not disturb the separation process. For example, an ECPP column for the separation D_2 from aqueous acidic solution may contain palladium as the separating electrode since it reacts reversibly with hydrogen (*15*).

A reference electrode may be also included in order to monitor or control the electrical potential of the separating electrode.

Two immobilization processes of the isotopes are considered in this work. Each requires a different treatment.

A) Electroadsorption. In this case the species are electroadsorbed at the double-layer region (*16*) of the electrode providing that an electric potential in the proper range is applied. Since only a monolayer is adsorbed and the relaxation time of the double layer is very short (*17*), the bound material is in equilibrium with the solution. The definition of α presented in Eq. (1) is thus valid.

B) Electrodeposition. In this case an electroactive species such as a metal ion is deposited as a new phase by electron exchange with the electrode. The isotope effect in this case may originate from the phase transformation or from a change in the oxidation state of the species (as in the case of uranium isotopes (*18*)). Since in this case the electrode is covered by a multilayer deposit (such as metal in the case of cations), it is assumed that the inner layers are no longer in equilibrium with the solution. The definition of α will thus be changed to

$$\alpha = \frac{Z}{1-Z} \quad \frac{dn_a^s}{dn_b^s} \tag{2}$$

where dn_a^s and dn_b^s are the momentary amounts of Isotopes a and b, respectively, deposited on the electrode at any time of the deposition process. The interlayer diffusion rate is assumed negligible in comparison with the rate of deposition.

2.2. The Concept of Column Division into "Cells"

The ECPP cycle considered in the present work consists of the following four consecutive steps (*3*). 1) Step R in which the electroactive species are attached to the surface of the electrode. 2) Step F in which the solution within the column is pushed in a forward direction. 3) Step O in which the species attached to the electrode are returned to the solution. 4) Step B in which the solution within the column is pushed backwards.

The other possible step combination equivalent to that is frequently applied to thermal parametric pumps, i.e., when Steps R and F and O and B are conducted simultaneously (*3*). This is not considered here since it leads to a rather complicated analysis.

In the coming discussion, the buildup mechanism of the isotopic concentration gradients will be outlined. The following simplifying assumptions are employed. 1) Plug flow is maintained during the flow Steps F and B; thus, dispersion processes are negligible. 2) Axial and transversial diffusion processes are negligible. 3) Interphase equilibrium is maintained between the electrode and the solution during Steps R, F, and B. 4) The top and bottom reservoirs have the same volume, $\Delta V = A\Delta L$, where ΔL is the solution displacement length at the flow steps and A is the column cross section. 5) There is a complete mixing of the solution in each reservoir.

The ECPP separation of Isotopes a and b is started with a column of uniform total isotopic concentration and composition expressed by g moles per unit of column length and Z_0, the mole fraction of a, respectively. The bottom reservoir contains a solution of volume ΔV while the top reservoir is empty. The isotopes are assumed to be in the form of cations. At Step R, a fraction m of the total concentration is bound to the working electrode (and thus becomes immobile) either by adsorption or by deposition as a result of the application of a potential difference between this electrode and the auxiliary electrode. The total concentration of the solution at the end of this step is $g(1-m)$. Since Isotope b is preferentially bound, the solution within the column is enriched with Isotope a, the mole fraction of which changes to Z_R.

At Step F the solution within the column is pushed forward by a relative displacement length Δl^* and the solution entering the column from the bottom reservoir carries the original mole fraction Z_0 and a total concentration, $g(1-m)$. Since plug flow and the absence of axial diffusion are assumed, the column is divided into two sections ("cells") with different isotopic composition as shown in Fig. 1. At the bottom, a cell of length Δl,

*$\Delta l = \Delta L/L = \Delta V/V$, where L is the column length and V is the void volume of the column.

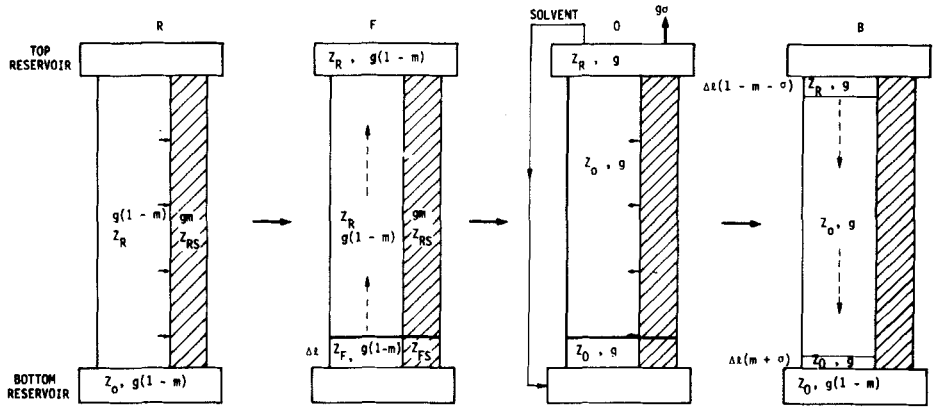

FIG. 1. The ECPP column at each of the four basic steps in a cycle. The division of the column into "cell" after the first cycle is shown. The cross-hatched area indicates the electrode, the open area indicates the solution, the full arrow indicates isotope movement, and the dashed arrow indicates solution movement.

the solution and electrode composition (Z_F and Z_{FS}, respectively) of which results from equilibration between the entering solution and the fraction electrodeposited at Step R. The second cell, i.e., the remainder of the column, carries the same solution and electrode composition as at the end of Step R (Z_R and Z_{RS}, respectively). The same solution is now also contained within the top reservoir.

At Step O the entire electrodeposit is returned to the solution by applying a reverse potential difference to the electrodes. The total concentration in the solution throughout the column and the isotope composition in the upper cell are restored, but at the lower cell the mole fraction of a (Z_O) becomes smaller than that in the upper cell and top reservoir. An isotopic concentration gradient exists now along the column. During this step, a fraction σ of ΔV which carries the original total concentration and mole fraction Z_R can be removed as a product from the top reservoir solution. This can be done only after a proper amount of solvent is removed (e.g., by distillation) from this reservoir in order to increase the total concentration to g.

At Step B the solution is pushed backward through the column. The displacement length is now $\Delta l\ (1 - m - \sigma)$, i.e., shorter than in Step F due to product withdrawal and solvent removal from the top reservoir. According to the assumptions made for Step F and as shown in Fig. 1, the solution phase within the column will be divided into three sections of different lengths and mole fractions ($Z_R > Z_0 > Z_O$) at the end of the first cycle.

Following the scheme outlined above, it may be seen that after $1/\Delta l(m + \sigma)$ cycles the solution phase along the column will be evenly divided into $N = 1/\Delta l$ cells of length Δl and each cell into $N' = 1/(m + \sigma)$ subcells of length $(m + \sigma)\Delta l$, as shown in Fig. 2.

2.3. Modes of Operation

Two modes of operation may be considered. In the first one, the total reflux mode, no product is withdrawn from the top reservoir and $\sigma = 0$. The excess solvent removed from this reservoir at Step O must be transferred to the bottom reservoir in order to keep the total concentration there at its original value, $g(1 - m)$. The isotope concentration gradients become more prominent as the cycles proceed until steady state is reached.

In the second mode the column is fed at a certain location along the column with a solution carrying the initial isotopic composition and total

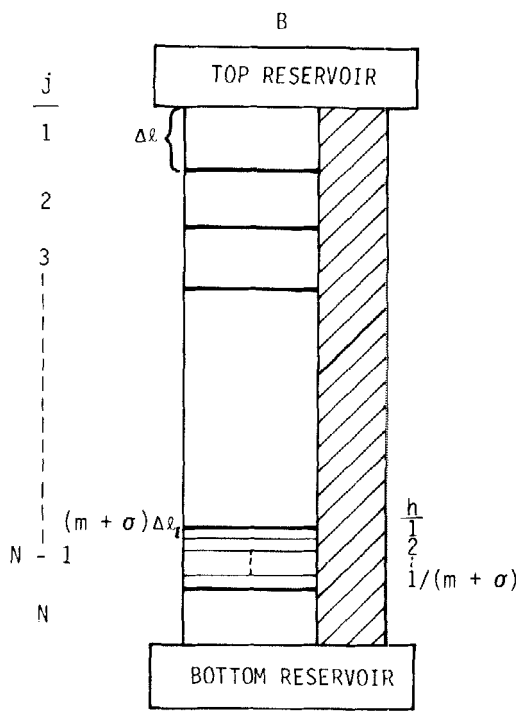

FIG. 2. "Cell" structure of the ECPP column at the end of $1/\Delta l(m + \sigma)$ cycles.

concentration, while isotopically enriched products are withdrawn from the top and bottom reservoirs.

In this work the bottom reservoir is chosen as the feed location since, as will be shown later, it provides a mathematical convenience.

2.4. Mass Balance Equations

Simple mass balance considerations for each one of the four steps at any cycle number, i, lead to the following equations:

Step R,

$$Z^{j,h}_{(i-1)B} = (1 - m)\, Z^{j,h}_{iR} + mZ^{j,h}_{iRS} \tag{3.1}$$

Step F,

$$(1 - m)\, Z^{j+1,h}_{iR} + mZ^{j,h}_{iRS} = (1 - m)Z^{j,h}_{iF} + mZ^{j,h}_{iFS} \tag{3.2}$$

$$(1 - m)Z_0 + mZ^{N,h}_{iRS} = (1 - m)Z^{N,h}_{iF} + mZ^{N,h}_{iFS} \tag{3.3}$$

$$Z^{T}_{if} = (m + \sigma) \sum_{h=1}^{N'} Z^{1,h}_{iR} \tag{3.4}$$

Step O,

$$Z^{j,h}_{iO} = (1 - m)Z^{j,h}_{iF} + mZ^{j,h}_{iFS} \tag{3.5}$$

Step B,

$$\left.\begin{aligned} Z^{1,h}_{iB} &= Z^{T}_{iF} \\ Z^{j,h}_{iB} &= Z^{j-1,h+1}_{iO} \end{aligned}\right\} \text{ where } h = 1, \ldots, (N' - 1) \tag{3.6, 3.7}$$

$$Z^{j,h}_{iB} = Z^{j,1}_{iO}, \qquad \text{where } h = N' \tag{3.8}$$

$$(1 - m)Z^{B}_{iB} = \frac{m + \sigma}{1 - m - \sigma} \sum_{h=2}^{N'} Z^{N,h}_{iO} \tag{3.9}$$

In these equations, $Z^{j,h}_{iR}$, $Z^{j,h}_{iF}$, $Z^{j,h}_{iO}$, and $Z^{j,h}_{iB}$ denote the mole fractions of Isotope a in the solution at cell j, subcell h, and cycle number i at the end of steps R, F, O, and B, respectively; $Z^{j,h}_{iRS}$ and $Z^{j,h}_{iFS}$ the corresponding mole fractions on the electrode; and Z^{T}_{iF} and Z^{B}_{iB} the mole fractions of a at the top and bottom reservoir, respectively, calculated by averaging over the

appropriate number of subcells. This procedure is required since a perfect mixing of the solution in each reservoir was assumed previously.

2.5. The Effective Separation Factor

The net result of the complete four-step ECPP cycle at any location j,h along the column is a forward flow of a solution of composition $Z_{iR}^{j,h}$ and a backward flow of a solution composition $Z_{iB}^{j,h}$. Although the same fluid is involved in both flows, the ECPP resembles a countercurrent separation process. In both cases there is a material exchange between the two streams that provides the basic separation effect. In the ECPP process, material exchange proceeds through the solid electrode bed via Steps R and O.

We may define the effective separation factor for the pseudocountercurrent ECPP as

$$\beta = \frac{Z_{iR}^{j,h}}{1 - Z_{iR}^{j,h}} \Big/ \frac{Z_{(i-1)B}^{j,h}}{1 - Z_{(i-1)B}^{j,h}} \tag{4}$$

Considering the differences between the adsorption and the deposition processes outlined in Section 2.1, β should be treated for each case separately. In the case of adsorption, the use of Eqs. (1), (3.1), (4), and the approximation $\alpha \simeq 1$ gives

$$\beta_a = 1 + m(\alpha - 1) \tag{5}$$

where β_a is the adsorption effective separation factor. Since $1 > m > 0$, it is clear that $1 < \beta_a < \alpha$.

In the case of deposition, the following considerations are employed. Mass balance during Step R requires that

$$\begin{aligned} dn_a^s &= -dn_a \\ dn_b^s &= -dn_b \end{aligned} \tag{6}$$

but

$$\begin{aligned} n_a &= g(1 - m)Z \\ n_b &= g(1 - m)(1 - Z) \end{aligned} \tag{7}$$

where n_a and n_b are the number of moles of a and b in the solution, respectively. Differentiation of Eqs. (7) and introduction of the result and Eqs. (6) into Eq. (2) lead to

$$(\alpha - 1)\frac{dm}{1-m} = \left(\frac{1}{1-Z} + \frac{\alpha}{Z}\right)dZ \tag{8}$$

Integration of Eq. (8) over the intervals $[0, m]$ and $[Z^{j,h}_{(i-1)B}, Z^{j,h}_{iR}]$ yields

$$(1-m)^{(1-\alpha)} = \left(\frac{Z^{j,h}_{(i-1)B}}{Z^{j,h}_{iR}}\right)^{\alpha}\left(\frac{1-Z^{j,h}_{iR}}{1-Z^{j,h}_{(i-1)B}}\right) \tag{9}$$

The right-hand side of Eq. (9) is expanded into a Taylor series near $\alpha = 1$, and by assuming $\alpha \simeq 1$ we get

$$\beta_d = (1-m)^{(1-\alpha)} \tag{10}$$

where β_d is the deposition effective separation factor.

In Fig. 3, β_a and β_d are depicted as a function of m. It is evident that as m decreases, β_a and β_d approach the same values. This is due to the fact that in the case of deposition, at very small values of m, the coverage of the electrode approaches a monolayer as in the case of adsorption. Thus the interphase isotopic equilibrium mechanism is the same for both cases. On the other hand, when m increases, β_d becomes much larger than α while β_a does not exceed this value.

2.6. Steady-State Isotopic Composition along the Column

The cell model outlined above and the presentation of parametric pumping as a countercurrent process provide a pathway for the calculation of steady state isotopic concentration profiles along the column.

The use of the mass balance Eqs. (3.1)–(3.9) for this purpose is not straightforward since in cases where $(m + \sigma)$ is not a simple fraction, the buildup of subcells within a cell becomes complicated. This would introduce severe complexities in the treatment of these equations since the repetitive behavior of the system upon completion of a cycle will no longer be valid.

This difficulty can be overcome if it is assumed that each B step is followed by an imaginary mixing step in which the content of each cell is completely mixed and any subcell hyperstructure is destroyed at the end of each cycle.

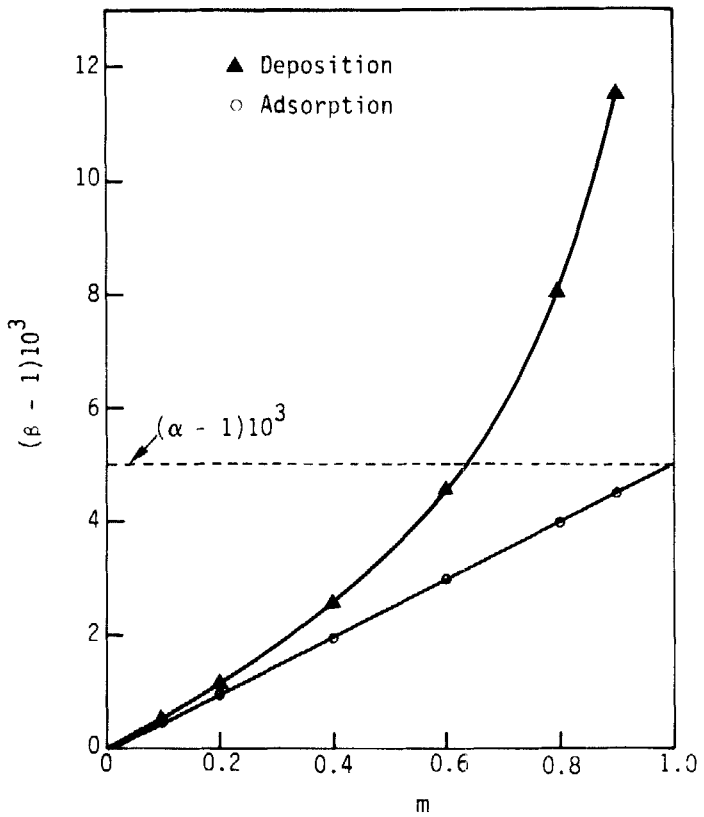

FIG. 3. The effective separation factors for deposition and adsorption as a function of m; $\alpha = 1.005$.

No mixing between cells is allowed. The addition of a mixing step extremely simplifies the cell structure of the column. In this case each cycle is started with a column divided into N cells each of length Δl and at the end of Step B each cell is divided further into two subcells of lengths $\Delta l\,(1 - m - \sigma)$ and $\Delta l(m + \sigma)$ as shown in Fig. 4. An additional mass balance equation has to be considered, namely,

$$\bar{Z}^j_{iB} = (1 - m - \sigma)Z^{j,1}_{iB} + (m + \sigma)Z^{j,2}_{iB} \tag{11}$$

where $\bar{Z}^j_{iB}$ is the average mole fraction of a at Cell j due to the mixing of the content of Subcells j,1 and j,2.

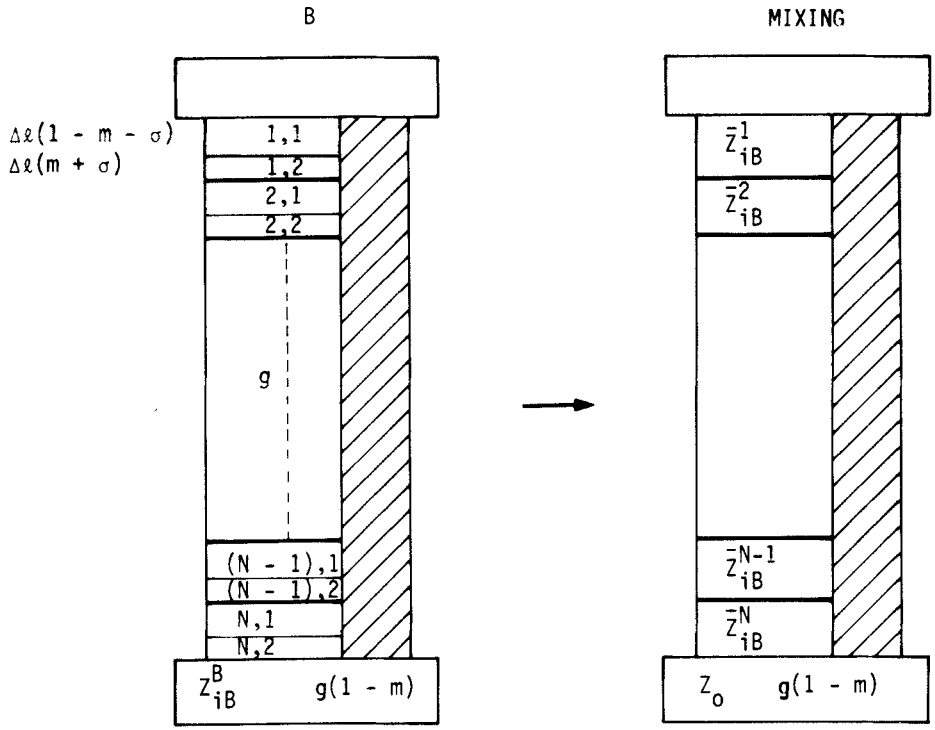

FIG. 4. "Cell" structure of the ECPP column at the end of Step *B* and the mixing step.

The simplification of the cell structure of the column is not the only advantage gained by the introduction of the mixing step. As will be shown later, the mixing step has the same effect on the concentration gradients as if dispersive processes (which were neglected in the discrete cell analysis) are considered.

It is now possible to derive a one-dimensional, continuous, mass balance equation by the use of the discrete Eqs. (3) and (11), providing that Δl is chosen small enough, and transversial dispersion processes are neglected. According to the procedure outlined in Appendix I, we get

$$\frac{\partial Z}{\partial n} = [(\beta - 1)(1 - m) + \sigma]\Delta l \frac{\partial Z}{\partial l} - \left[\beta(m + \sigma)(1 - m)(\Delta l)^2 + \frac{D\tau}{L^2}\right]\frac{\partial^2 Z}{\partial l^2}$$

"separation" "product" "mixing" "dispersion" (12)

As may be observed, the right-hand side of Eq. (12) is composed of four terms originating from different flux contributions. 1) An inherent mixing flux which results from the fact that at the end of Step F, the composition of the solution and the electrode at any cross section along the column do not justify α. Therefore, upon equilibration, the solution is slightly depleted of Isotope a, a process that may be represented by a dispersionlike flux term since it affects the concentration gradient of a. 2) An axial dispersion flux. 3) A separation flux accounted for the flux of Isotope a due to the separation effect (this term vanishes when $\beta = 1$). 4) A product flux which is in the same direction as the separation flux.

Equation (12) is now solved for steady-state conditions by placing $(\partial Z/\partial n) = 0$ and using the following boundary conditions, at $l = 0$ $(j = 1)$,

$$\partial Z/\partial l = KZ \tag{13}$$

where

$$K = \frac{(1 - m - \sigma)(1 - \beta)}{\beta(m + \sigma)(1 - m)\Delta l + \dfrac{D\tau}{L^2 \Delta l}} \tag{13a}$$

and at $l = 1$ $(j = \mathrm{N})$,

$$Z = Z_0 \tag{14}$$

The derivation of Eq. (13) is outlined in Appendix II. The steady-state solution of Eq. (12) with boundary conditions (13) and (14) is

$$Z = Z_0 \frac{e^{-Rl} - 1 - (R/K)}{e^{-R} - 1 - (R/K)} \tag{15}$$

where R is defined as

$$R = \frac{[(\beta - 1)(1 - m) + \sigma]\Delta l}{\beta(m + \sigma)(1 - m)(\Delta l)^2 + \dfrac{D\tau}{L^2}} \tag{15a}$$

Equation (15) provides a tool for the calculation of the isotopic concentration gradient along the column at steady state. Thus the ultimate enrichment level as a function of the system parameters m, σ, α, and Δl can be obtained.

Moreover, as will be shown later, it also provides a way for the optimization of the separation process.

It is important at this stage to point to the similarity between Eq. (12) and the transport equation derived for the countercurrent isotope separation process. As presented by London (*19*) the latter equation contains three flux terms related to the separation effect, internal mixing, and dispersion, as in Eq. (12).

3. RESULTS AND DISCUSSION

The set of mass balance Eqs. (3) was inserted into a computer program in order to simulate the ECPP isotope separation process in a step-wise manner according to the cell model. When Eq. (11) is inserted into this program, the mixing step is taken into account and the analysis provides a more realistic view of the process. Moreover, in this case it is also possible to compare between the discrete cell model and the continuous analysis and to test the validity of Eqs. (12) and (15).

The results of the computer runs for the cell model without considering the mixing step are depicted in Figs. 5 and 6 (α was arbitrarily taken to be 1.005 in these calculations). The enrichment, y_T, at the top reservoir, defined as

$$y_T = \frac{Z_T}{Z_0} - 1 \tag{16}$$

is given in Fig. 5A for the case of deposition as a function of the cycle number for several values of m. For a certain m, y_T increases as the process proceeds and reaches a steady state value when the separation effect is exactly compensated by the inherent mixing effect (these are the only effects taking part in this idealized model at total reflux). The steady-state enrichment, $(y_T)_{SS}$, is depicted in Fig. 5B as a function of m for the deposition and adsorption cases. It is evident that for the same set of conditions, $(y_T)_{SS}$ increases much more rapidly with m in the case of deposition as compared to the case of adsorption. This discrepancy is understood in view of the difference in the behavior of β_d and β_a as shown in Fig. 3.

In Fig. 6, y_T is shown as a function of the cycle number for different Δl values. As in the case of desalination by ECPP (Eq. 3), $(y_T)_{SS}$ increases significantly and the rate of approach to steady state is smaller as Δl decreases.

The rate of approach to steady state is also a function of m. As may be observed in Fig. 5A, this rate has a maximum at $m = 0.5$, a behavior which

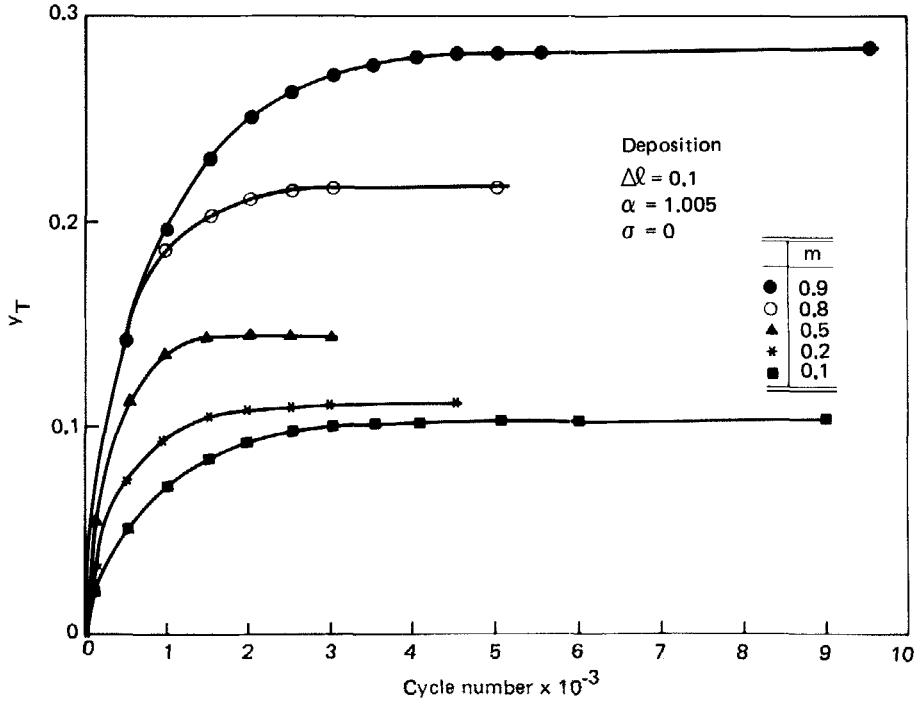

FIG. 5a. y_T as a function of cycle number for different m values and constant Δl. Stepwise calculation.

may be attributed to the balance between the inherent mixing and the separation effects. A close inspection of Eq. (12) reveals that the separation term is linear while the inherent mixing term is a parabolic function of m with a maximum value at $m = 0.5$ when $\sigma = 0$. The latter effect will balance the former most rapidly at its maximum value, thus resulting in the highest rate of approach to steady state.

The effect of σ on $(y_T)_{SS}$ is depicted in Fig. 7 in terms of the relative deviation from y_{SS}^{TR}, the enrichment at steady-state total reflux. As may be expected, $(y_T)_{SS}$ attains its highest value at total reflux ($\sigma = 0$) and decreases significantly as σ increases. The relative deviation from total reflux increases as both m and Δl decrease.

The effect of the introduction of the mixing step to the cell model is shown in Fig. 8 where the isotopic mole fraction profile along the column at steady state (local mole fractions at steady state are expressed as $y_{SS} = (Z/Z_0) - 1$)

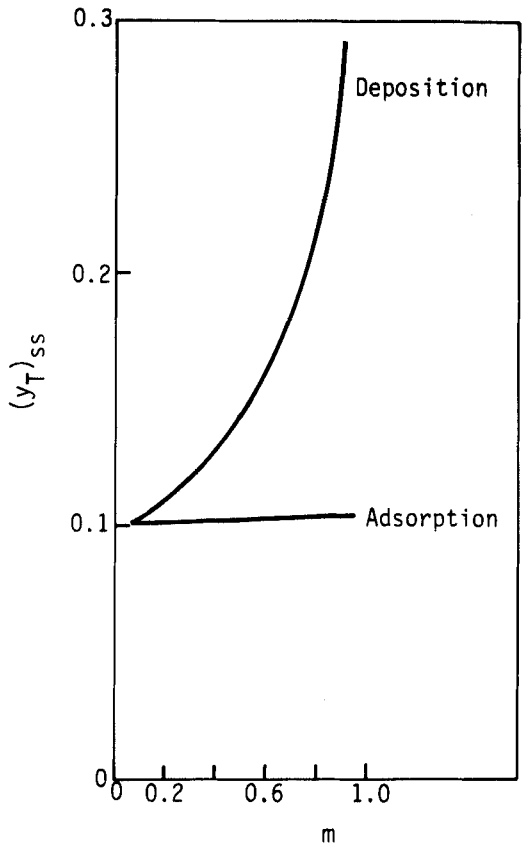

FIG. 5b. $(y_T)_{SS}$ as a function of m for deposition and adsorption. Stepwise calculation.

calculated without considering this step is compared with the profile calculated when this step was taken into account. The reduction of mole fractions along the column in the presence of mixing is justified in view of the similarity between the mixing step and dispersion processes as discussed in Section 2.

The mole fraction profiles at steady state as obtained by the stepwise calculation when the mixing step is taken into account are compared in Fig. 9 to the profiles calculated by means of Eq. (15) when the dispersion terms are not considered (i.e., D is taken to be zero; it should be recalled that in this case, dispersion and mixing processes are represented only by the mixing step which was considered in the derivation of Eq. 15). It is evident that there

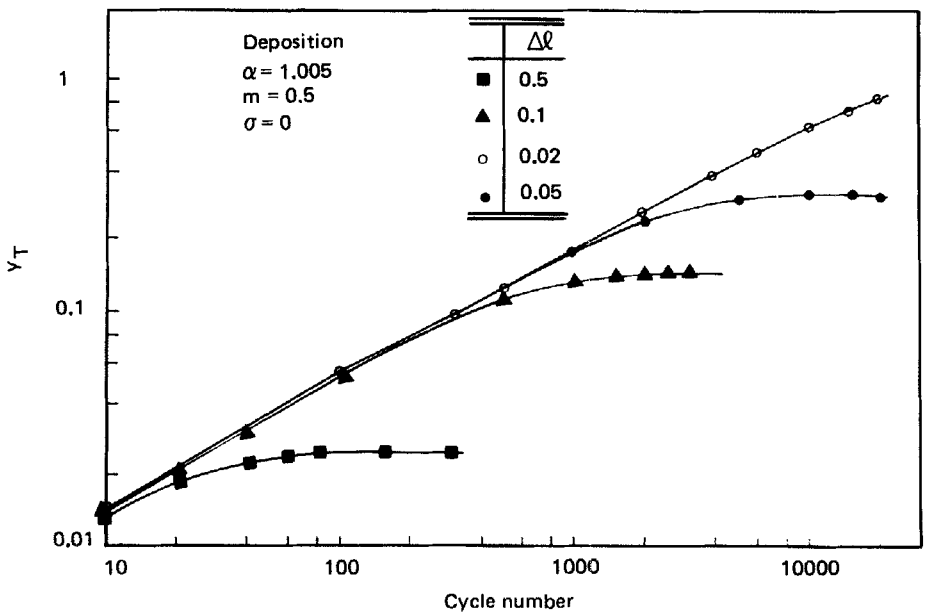

FIG. 6. y_T as a function of cycle number for different Δl values and constant m. Stepwise calculation.

is an excellent agreement between the two modes of calculation at a wide range of Δl values.

As depicted in Fig. 10, calculations by means of Eq. (15) show a considerable reduction in isotopic concentrations when the dispersion terms are taken into account.

The Number of Theoretical Plates

Equation (15) provides a means for the estimation of the number of theoretical plates which is a measure for the number of enrichment stages along the separating column at total reflux. In analogy with the height of the equivalent theoretical plate (HETP) as defined for countercurrent processes (*19*), the HETP for the ECPP is a section of a column length which reproduces the basic separation factor, α. Thus,

$$\text{HETP} = l_1 - l_2 \tag{17}$$

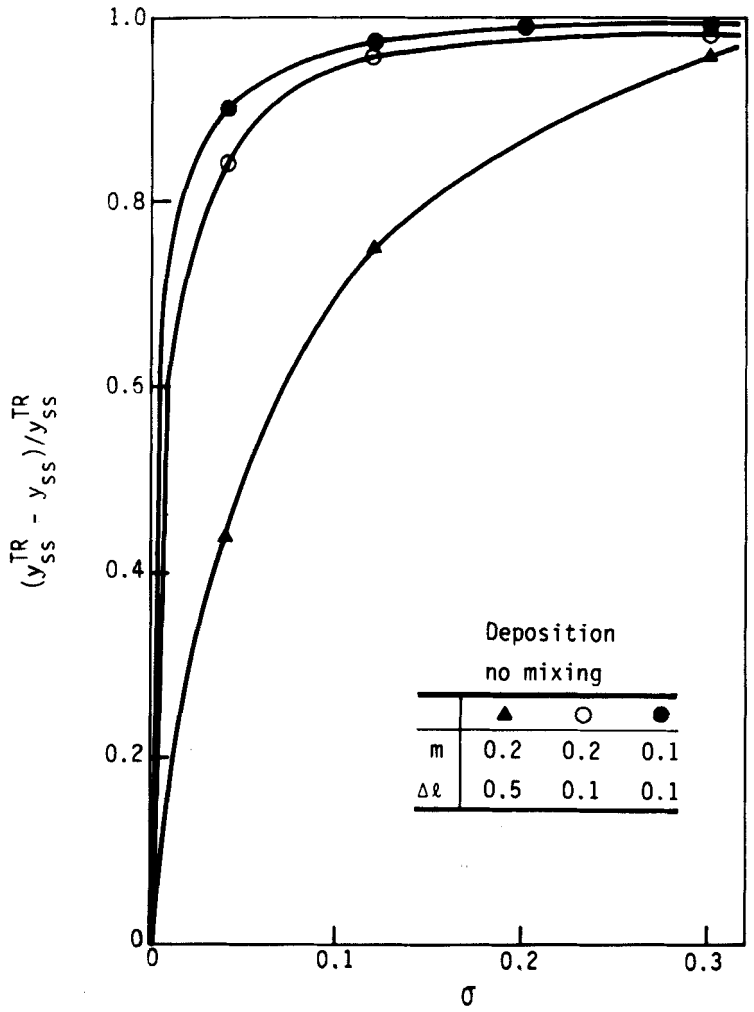

FIG. 7. The relative deviation of $(y_T)_{SS}$ from the total reflux value as a function of σ for various conditions. Stepwise calculation.

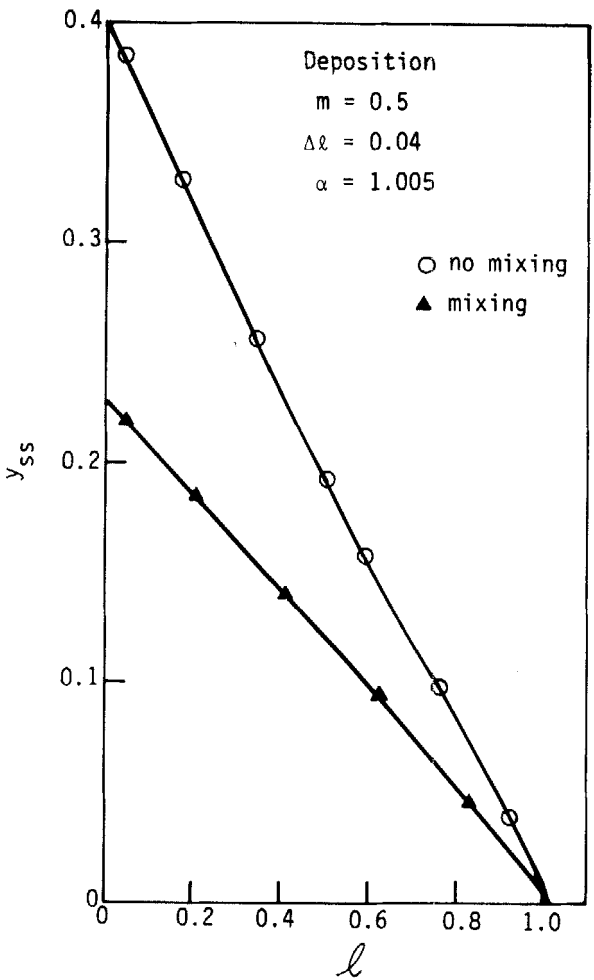

FIG. 8. y_{SS} as a function of column length calculated in the presence of mixing step as compared to the case when no mixing step is introduced.

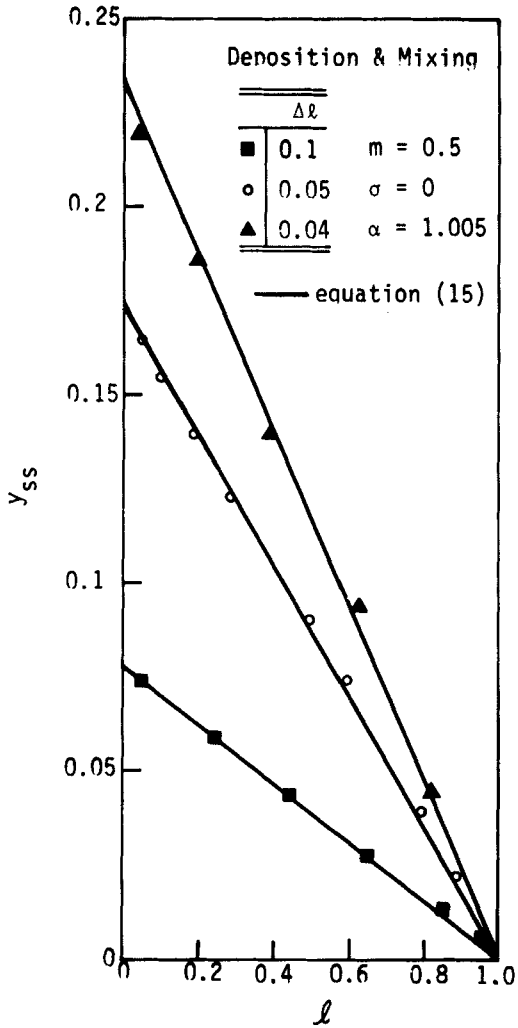

FIG. 9. y_{SS} as a function of column length. A comparison of the stepwise calculation with the mixing step and the calculation by means of Eq. (15).

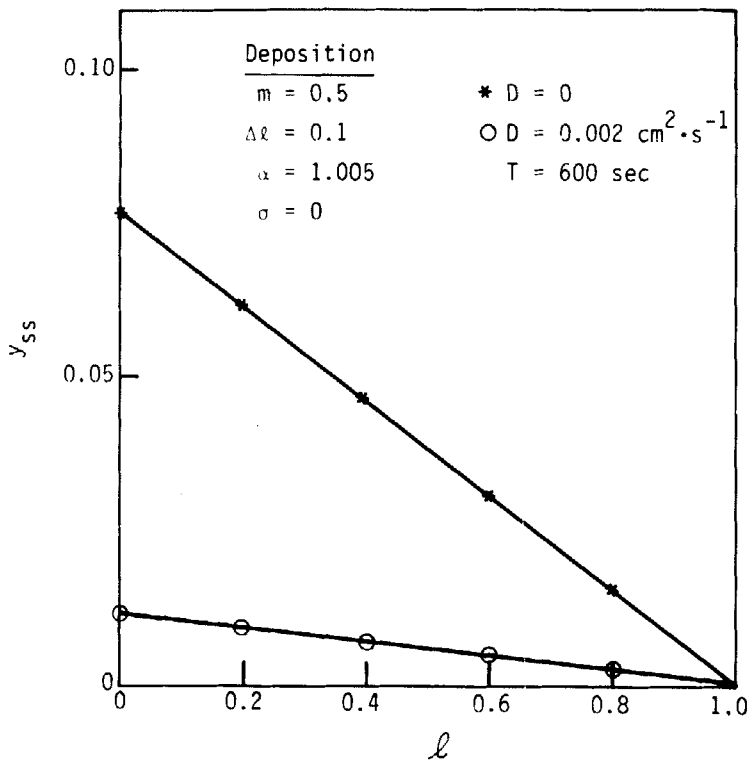

FIG. 10. The effect of the addition of the dispersion terms in Eq. (15) on y_{SS} profile.

where l_1 and l_2 are the locations along the column characterized respectively by the isotopic mole fractions Z_1 and Z_2 which obey

$$\alpha = \frac{Z_1}{1 - Z_1} \Big/ \frac{Z_2}{1 - Z_2} \tag{18}$$

Z_1 and Z_2 are calculated from Eq. (15) for $\sigma = 0$. By assuming $\alpha \simeq 1$, we get

$$\text{HETP} = \frac{1}{R} \ln \alpha \tag{19}$$

and the number of theoretical plates, N_H is

$$N_H = 1/\text{HETP} \tag{20}$$

The variations of N_H with Δl and m are shown in Figs. 11A and 11B for deposition and adsorption, respectively. It is clear that in both cases the effect of Δl is much stronger than the effect of m. In the case of adsorption the figure reveals that N_H does not vary with m. This behavior may be verified by inserting β_a from Eq. (5) into Eq. (19) and employing the approximations $\alpha \simeq 1$ and $\ln \alpha \simeq 1 - \alpha$. This results in

$$\text{HETP} = \Delta l \tag{21}$$

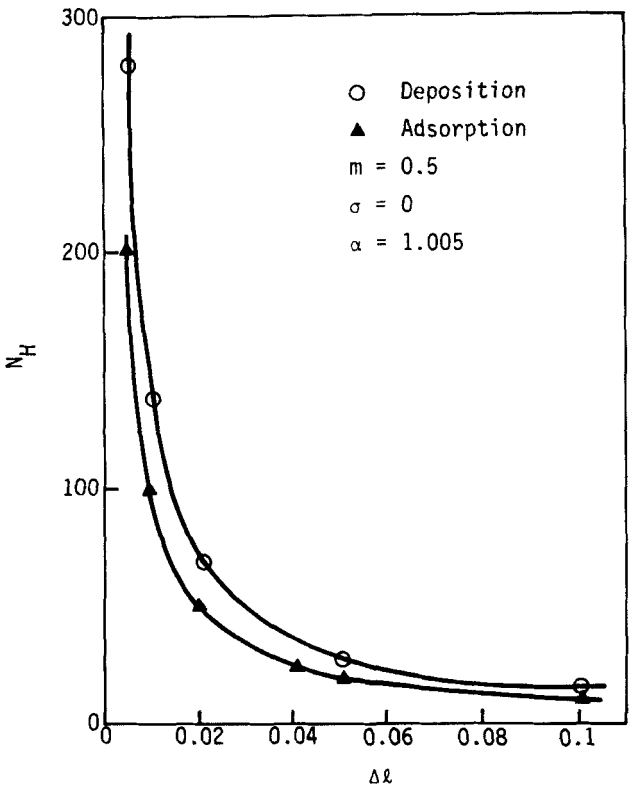

FIG. 11a. The number of theoretical plates as a function of Δl for deposition and adsorption.

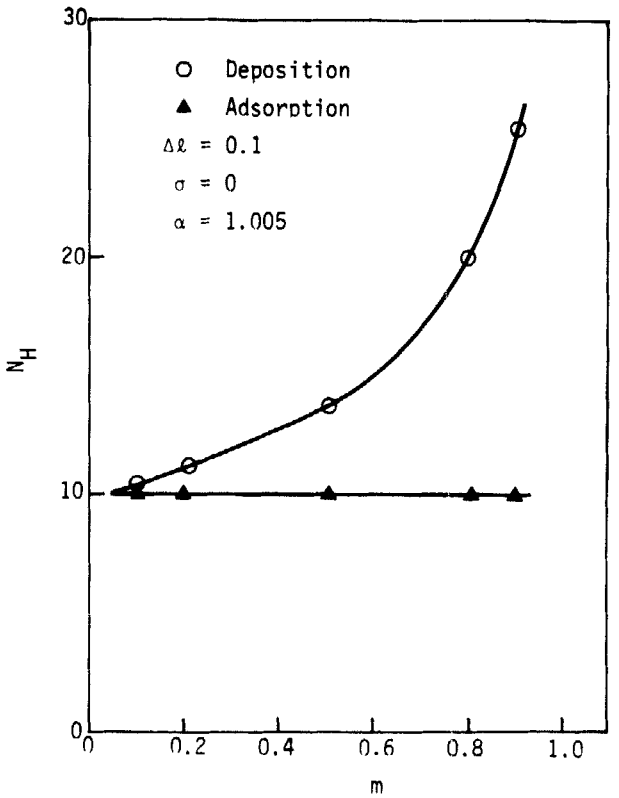

FIG. 11b. The number of theoretical plates as a function of m for deposition and adsorption.

Moreover, it can be shown from Eqs. (10) and (19) that if m is taken small enough, the HETP for the deposition process also equals Δl.

The Separation Work and Process Optimization

The separation work E is defined as (*19*)

$$E = J\left(\frac{dZ}{dl}\right)_{ss} \tag{22}$$

where J is the net flux of the isotope and $(dZ/dl)_{SS}$ is the steady-state mole fraction gradient in the solution. E becomes zero in two extreme cases: at total reflux when no product is withdrawn from the column and thus the net flux J is zero, and immediately at the beginning of the process when no concentration gradient is present. For the best performance of the separation device, the separation work should be kept at its highest value. It therefore provides the basis for the optimization of the process with respect to system parameters such as m, σ, and Δl.

The net flux J may be expressed as

$$J = \frac{g\sigma Z(0)}{\tau_\sigma} \tag{23}$$

where $Z(0)$ is the mole fraction at $l = 0$ and τ_σ is the duration of product withdrawal.

The concentration gradient is written as

$$(dZ/dl)_{SS} = Z(0) - Z_0 \tag{24}$$

since at steady state it is nearly linear as shown in Figs. 8 and 9.

Equations (23) and (24) are now introduced into Eq. (22), and $Z(0)$ is expressed by Eq. (15) to obtain

$$E_N = \frac{\sigma(R/K)(e^{-R} - 1)}{[(R/K) + 1 - e^{-R}]^2} \tag{25}$$

where

$$E_N = \frac{\tau_\sigma}{gZ_0^2} E \tag{25a}$$

The optimization procedure of E_N is demonstrated in Figs. 12 and 13. In Fig. 12, E_N is depicted as a function of m for various values of σ for the case of deposition. For each σ the curve shows an optimal value for E_N which, when drawn as a function of σ (Fig. 13), enables the extraction of σ_{opt} and the corresponding m_{opt}. In the specific case shown in the latter figures, E_N is calculated for $\Delta l = 0.02$ and $D = 0$. It is found that $m_{opt} = 0.5$ and $\sigma_{opt} = 0.02$ for adsorption and $m_{opt} = 0.71$ and $\sigma_{opt} = 0.01$ for deposition. When E_N is calculated as a function of Δl for any set of conditions, it is found that the largest value is obtained when Δl is close to zero. This is in

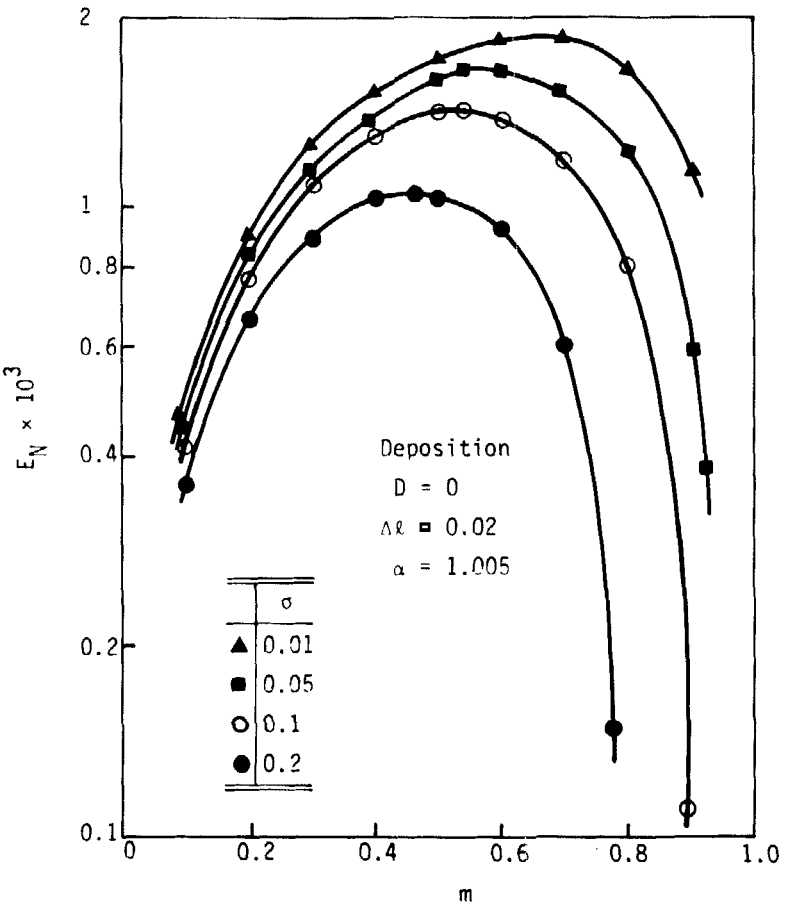

FIG. 12. The normalized separation work, E_N, as a function of m for different σ values.

agreement with the large effect of Δl on the concentration difference along the column as shown in Fig. 6 and on the number of theoretical plates as shown in Fig. 11. On the other hand, it should be recalled that a decrease in Δl results in a marked decrease in the rate of approach to steady state (Fig. 6). This effect was not taken into account in the derivation of Eq. (25) but has to be considered whenever optimization is studied. Another important parameter which has to be considered in the optimization procedure is the rate of deposition (or adsorption) of the isotopes at Step R. When the rate of deposition is very large, the isotope composition in the solution side of the electrode/solution interface may differ considerably from the bulk solution

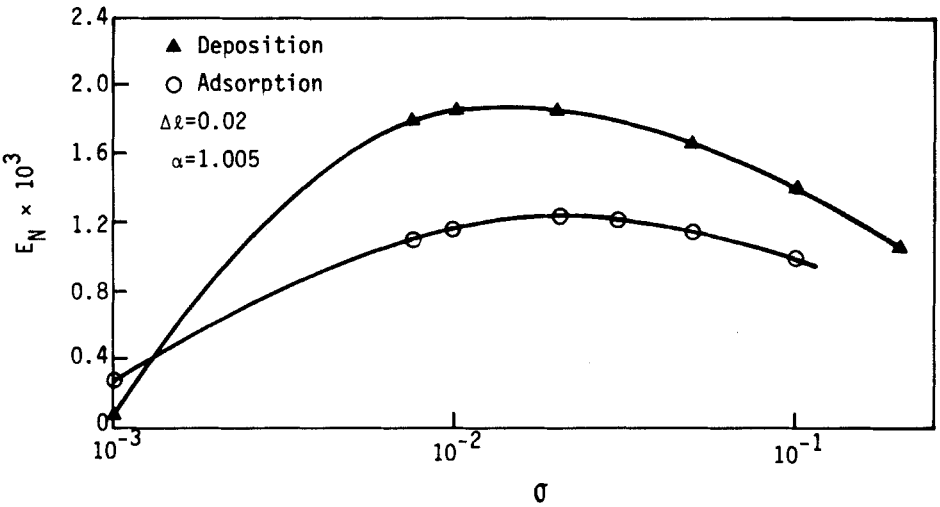

FIG. 13. The normalized separation work, E_N, at m_{opt} as a function of the corresponding σ.

due to the existence of an unstirred layer (*20*). Since Isotope *a* is bound preferentially to the electrode, the solution near the interface will be richer in Isotope *b* as compared to the bulk solution. Thus, if equilibrium is maintained at the interface, the basic separation effect will be reduced. Moreover, the separation factor α may be altered due to the existence of nonequilibrium processes at the interface.

The electric current which controls the rate of deposition at Step *R* should therefore be chosen to be small enough to avoid these effects.

In this case, unless solution flow rates at Steps *B* and *F* are taken to be small because of dispersion considerations, Step *R* becomes the limiting factor of the cycle duration. Step *O* may be very short since the electric current for dissolution can be much larger than the deposition current. This current is limited only by solvent decomposition considerations.

4. CONCLUSIONS

The application of the countercurrent concept is not restricted to ECPP but may be valuable to other forms of parametric pumping as well. The marked feature of the similarity between the two processes is that it enables a straightforward derivation of expressions for the isotopic concentration gradient at steady state for a process that is stepwise in nature. This

expression is of great importance for the prediction of the ultimate isotopic concentrations and for the optimization of the separation process.

APPENDIX I

Derivation of a Continuous Mass Balance Equation

By the use of Eqs. (3.2), (3.5), and (3.7) expressed properly according to the mixed cells model, Eq. (11) is converted to

$$Z^j_{iB} = (1 - m - \sigma)[(1 - m)Z^j_{iR} + mZ^{j-1}_{iRS}] + (m + \sigma)[(1 - m)Z^{j+1}_{iR} + mZ^j_{iRS}] \tag{A1}$$

Assuming $\beta \simeq 1$ (this is true for any m in the case of adsorption and if m does not exceed 0.95 in the case of deposition), an approximate expression is obtained for Eq. (4), namely:

$$Z^j_{iR} = \beta \bar{Z}^j_{(i-1)B} \tag{A2}$$

Equation (A2) is now placed in Eq. (3.1) thus:

$$mZ^j_{iRS} = [1 - \beta(1 - m)]\bar{Z}^j_{(i-1)B} \tag{A3}$$

The introduction of Z^j_{iR} and Z^j_{iRS} from Eqs. (A2) and (A3) into Eq. (A1) and rearrangment yields

$$\bar{Z}^j_{(i-1)B} - \bar{Z}^j_{iB} = [(\beta - 1)(1 - m) + \sigma](\bar{Z}^{j-1}_{(i-1)B} - \bar{Z}^j_{(i-1)B}) - \beta(m + \sigma)(1 - m)[(\bar{Z}^{j-1}_{(i-1)B} - \bar{Z}^j_{(i-1)B}) - (\bar{Z}^j_{(i-1)B} - \bar{Z}^{j+1}_{(i-1)B})] \tag{A4}$$

The differences of Z in Eq. (A4) can be converted into differentials if Δl is taken as a differential length and the cycle duration τ is considered as a differential time. Thus,

$$\bar{Z}^j_{(i-1)B} - \bar{Z}^j_{iB} = \frac{\partial Z}{\partial n} \tag{A5}$$

$$\bar{Z}^{j-1}_{(i-1)B} - \bar{Z}^{j}_{(i-1)B} = \Delta l \frac{\partial Z}{\partial l} \tag{A6}$$

and

$$(\bar{Z}^{j-1}_{(i-1)B} - \bar{Z}^{j}_{(i-1)B}) - (\bar{Z}^{j}_{(i-1)B} - \bar{Z}^{j+1}_{(i-1)B}) = (\Delta l)^2 \frac{\partial^2 Z}{\partial l^2} \tag{A7}$$

where n is the cycle number.

Expressions (A5), (A6), and (A7) are placed in Eq. (A4) together with an additional axial dispersion term, $(D\tau/L^2)(\partial^2 Z/\partial l^2)$, and Eq. (12) is obtained. D is the dispersion coefficient.

APPENDIX II

Derivation of the Boundary Condition at $l = 0$ ($j = 1$)

Equation (11) for $j = 1$ is

$$\bar{Z}^{1}_{iB} = (1 - m - \sigma) Z^{11}_{iB} + (m + \sigma) Z^{12}_{iB} \tag{A8}$$

By the use of Eqs. (3.6), (3.4), and (A2) we obtain

$$Z^{11}_{iB} = \beta \bar{Z}^{1}_{(i-1)B} \tag{A9}$$

and with Eqs. (3.7), (3.5), (3.2), (A2), and (A3),

$$Z^{12}_{iB} = \beta(1 - m)\bar{Z}^{2}_{(i-1)B} + [1 - \beta(1 - m)]\bar{Z}^{1}_{(i-1)B} \tag{A10}$$

At steady state,

$$\bar{Z}^{j}_{iB} = \bar{Z}^{j}_{(i-1)B} \tag{A11}$$

Equations (A9), (A10), and (A11) are now placed in Eq. (A8) and after rearrangement we obtain

$$(1 - m - \sigma)(1 - \beta)\bar{Z}^{1}_{iB} = \beta(m + \sigma)(1 - m)(\bar{Z}^{1}_{iB} - \bar{Z}^{2}_{iB}) \tag{A12}$$

Equation (13) is derived from Eq. (A12) by the conversion of $\bar{Z}_{iB}^{1} - \bar{Z}_{iB}^{2}$ to its differential form according to the considerations outlined in Appendix I and by the addition of a dispersion term $(\tau D/L^2 \Delta l)(\partial Z/\partial l)$.

REFERENCES

1. Y. Oren and A. Soffer, "Electrochemical Parametric Pumping," *J. Electrochem. Soc., 125*, 869 (1978).
2. Y. Oren and A. Soffer, "Water Desalination by Means of Electrochemical Parametric Pumping. I. The equilibrium properties of a batch unit cell," *J. Appl. Electrochem., 13*, 473 473 (1983).
3. Y. Oren and A. Soffer, "Water Desalting by Means of Electrochemical Parametric Pumping. II. Separation Properties of a Multistage Column," *Ibid., 13*, 489 (1983).
4. S. Kihara, "Analytical Chemical Studies on Electrode Processes by Column Coulometry. I. Basic Studies on the Column Electrode," *Electroanal. Chem., 45*, 31 (1973).
5. T. Fujinaga, "Electrolytic Chromatography and Coulometric Detection with the Column Electrode," *Pure Appl. Chem., 25*, 709 (1971).
6. J. O. Bockris and A. K. N. Reddy, *Modern Electrochemistry*, Vol. 2, Plenum, New York, 1970, pp. 1105, 1248; P. Gallone, in *The Encyclopedia of Electrochemistry* (C. A. Hampel, ed.), Reinhold, New York, 1964, p. 696.
7. E. Gileadi (ed.), *Electrosorption*, Plenum, New York, 1967.
8. T. J. Butts, R. Gupta, and N. H. Sweed, "Parametric Pumping Separations of Multicomponent Mixtures: An Equilibrium Theory, *Chem. Eng. Sci., 27*, 855 (1972).
9. R. L. Pigford, B. Baker, and D. E. Blum, "An Equilibrium Theory of the Parametric Pump," *Ind. Eng. Chem., Fundam., 8*, 144 (1969).
10. H. T. Chen, W. W. Lin, T. D. Stokes, and W. R. Fabisiak, "Separation of Multicomponent Mixtures Via Thermal Parametric Pumping," *AIChE J., 20*, 306 (1974).
11. Wu Xiang-Zhi and P. C. Wankat, "Continuous Multicomponent Parametric Pumping," *Ind. Eng. Chem., Fundam., 22*, 172 (1983).
12. K. Weaver and C. E. Hamrin, "Separation of Hydrogen Isotopes by Heatless Adsorption," *Chem. Eng. Sci., 29*, 1873 (1974).
13. H. G. Schroeder and C. E. Hamrin Jr., "Separation of Boron Isotopes by Direct Mode Thermal Parametric Pumping," *AIChE J., 21*, 807 (1975).
14. G. Grevillot and D. Tondeur, "Equilibrium Staged Parametric Pumping. I," *AIChE J., 22*, 1055 (1976); II, *Ibid., 23*, 840 (1977); G. Grevillot, III, *Ibid., 26*, 120 (1980).
15. F. A. Lewis, *Palladium–Hydrogen System*, Academic, New York, 1967.
16. P. Delahay, *Double Layer and Electrode Kinetics*, Wiley-Interscience, New York, 1963.
17. M. Yaniv and A. Soffer, "The Transient Behavior of an Ideally Polarized Porous Carbon Electrode at Constant Charging Current," *J. Electrochem. Soc., 123*, 506 (1976).
18. Y. Fujii, J. Fukuda, and H. Kakihana, "Isotope Effects in U(IV)–U(VI) Exchange Reaction," *J. Nucl. Sci. Technol., 15*, 745 (1978).
19. H. London (ed.), *Separation of Isotopes*, Newnes, London, 1961.
20. V. G. Levich, *Physicochemical Hydrodynamics*, Prentice-Hall, Englewood Cliffs, New Jersey, 1962.

Received by editor February 24, 1984